A UNIFIED APPROACH FOR IN-PLANE AND OUT-OF-PLANE CONSTRAINT ANALYSIS IN LINEAR ELASTIC CRACKED PLATES

E. Giner[1], D. Fernández Zúñiga[2], J. Fernández Sáez[3], A. Fernández Canteli[2]

[1]Dpto. de Ingeniería Mecánica y de Materiales-CITV, E.T.S. de Ingenieros Industriales
Universidad Politécnica de Valencia, Camino de Vera s/n, 46022 Valencia
E-mail: eginerm@mcm.upv.es

[2]Dpto. de Construcción e Ingeniería de Fabricación, E.P.S. de Ingeniería de Gijón,
Universidad de Oviedo, Campus de Viesques, 33203 Gijón.
E-mail: afc@uniovi.es

[3]Dto. de Mecánica del Medio Continuo y Análisis Estructural, Escuela Politécnica Superior,
Universidad Carlos III, Avda. Universidad 30, 28911 Leganés, Madrid.
E-mail: ppfer@ing.uc3m.es

ABSTRACT

The influence of the loss of constraint on the apparent fracture toughness, although early recognised, has not been adequately addressed up to present, especially in what concerns the out-of-plane case. In this paper, a tensor concept of the stress intensity and, in particular, of the first two terms of the Williams expansion is used with the aim of extending the concept of the conventional biparametric approaches to the analysis of the loss of constraint under general conditions encompassing both the in-plane and out-of-plane constraints. Based on analytical relations developed elsewhere, the components t_{11} and t_{33} of the t_{ij} tensor in the midplane of crack plates are numerically found by means of FE calculations, as well as their through-thickness variation along the crack front. The analyses are performed under different in- and out-of-plane constraint situations arising from different specimen thicknesses B, crack depth ratios a/W and Poisson coefficients ν, proving the numerical validity of the theoretical derivations.

KEY WORDS: *T*-stress, out-of-plane constraint, stress intensity tensor, constraint functions, Williams expansion.

1. INTRODUCTION

The increase of the apparent fracture toughness due to the loss of constraint has been recognized in the past in a number of theoretical and experimental works. In the case of the in-plane constraint, this effect has been traditionally explained as a result of the elastic *T*-stress giving rise, both in the LEFM [1] and EPFM [2], to the so-called two-parameter approaches, by considering the elastic *T*-stress as a reference magnitude. Nevertheless, this approach does not provide a definitive answer to the problem. Those studies are, in general, performed using specimen thicknesses greater than $B_{\min}$, what, according to the ASTM and ESIS standards, ensures plane strain conditions. As a consequence, the out-of-plane dimension of the constraint has been neglected. This is characterized by the presence of an often unconsidered out-of-plane t_{33} stress, as well as by the variation of the t_{11} stress, i.e. the conventional *T*-stress, as a result of the specimen thickness. Further, other parameters, as the crack depth a/W, typically identified with in-plane constraint effects, may also cause a significant variation of the out-of-plane stress t_{33}.

In previous works [3], a tensor approach based on Williams expansion is suggested to define the stress and strain state near the crack front. Sustained by analytical derivations and numerical calculations it is proved the independence of the structure of the stress intensity tensor k_{ij} with respect to the specimen thickness. The tensor k_{ij} allows to ascertain that the increase of the apparent fracture toughness due to the loss of constraint has to be assigned to the influence of higher order terms of the stresses.

In particular, this influence is assigned to the constraint tensor t_{ij}, identified as the Williams constant term tensor since it is independent of the radial distance r. The consideration of the stress intensity tensor k_{ij} and the so-called constraint curves ψ_{ij} [3] (see Section 3.3) enable us to demonstrate the correlation between the loss of constraint and the specimen thickness, and hence the necessity of considering the whole t_{ij} tensor, particularly its t_{33} component. This allows to tackle the general constraint problem under a unified approach, comprising both the in-plane and out-of-plane constraints. Current treatments of the constraint

problem contribute to a misleading identification of triaxiality with constraint that does not help to correctly establish the fracture criterion and the effect of thickness on the apparent fracture toughness.

In this work, numerical calculations are performed aiming at illustrating the influence of the specimen thickness on the t_{11} stress, i.e. the T-stress, and on the t_{33} stress and their relation to the out-of-plane strain ε_{33}. Analytical relations regarding the stress and strain tensor field at the crack front are used to numerically calculate the out-of plane stress component t_{33} and the T-stress t_{11}. This is accomplished through finite element analyses for different configurations and the results demonstrate the limitations of current approaches. This should contribute to the basic knowledge of the in- and out-of-plane constraints as a whole, paving the way to more general new fracture criteria.

2. THE TENSOR t_{ij} AS A MEASURE OF CONSTRAINT

The analytical derivations developed in [3], based on strain relations prevailing at the crack front of mode-I specimens, prove that the out-of-plane component k_{33} of the stress intensity tensor k_{ij} (defined as $k_{ij}(z;B) = K_1(z;B)\, f_{ij}(\theta)\big|_{\theta_{cr}}$) at the midplane of the specimen normal to the crack plane is given by

$$k_{33}(z;B) = \nu(k_{11}(z;B) + k_{22}(z;B)), \tag{1}$$

irrespective of the specimen thickness including the two limiting cases $B \to 0$ and $B \to \infty$. This necessarily implies the singular behaviour of σ_{33} along the crack front. In addition, the component $k_{33}(z;B)$ equals $2\nu K_I(z;B)$, leading to the following stress intensity tensor:

$$k_{ij}(z;B) = \begin{pmatrix} K_1(z;B) & 0 & 0 \\ 0 & K_1(z;B) & 0 \\ 0 & 0 & 2\nu K_1(z;B) \end{pmatrix}, \tag{2}$$

what demonstrates the independence of the k_{ij} structure with respect to the constraint level. Contrary to what is often found in the literature, Eq. (1) does not imply plane strain conditions at the crack front since $\varepsilon_{33} \neq 0$ and ε_{33} varies along the crack front. Furthermore, the following relation between out-of-plane strain ε_{33} at the crack tip and the components of t_{ij} has been found

$$\begin{aligned} \varepsilon_{33}(z,r;B)\big|_{r=0} &= \lim_{r\to 0} \frac{\sigma_{33}(z,r;B) - \nu\,(\sigma_{11}\nu - \sigma_{22}(z,r;B))}{E} \\ &= \frac{t_{33}(z;B) - \nu\, t_{11}(z;B)}{E} \end{aligned} \tag{3}$$

because the singular terms of σ_{ij} must cancel out to avoid a singular behaviour of ε_{33} at midplane. The corresponding tensor t_{ij} is given by

$$\begin{aligned} t_{ij}(z;B) &= \begin{pmatrix} t_{11}(z;B) & 0 & 0 \\ 0 & 0 & 0 \\ 0 & 0 & t_{33}(z;B) \end{pmatrix} \\ &= \begin{pmatrix} t_{11}(z;B) & 0 & 0 \\ 0 & 0 & 0 \\ 0 & 0 & E\varepsilon_{33}(z;B) + \nu\, t_{11}(z;B) \end{pmatrix} \end{aligned} \tag{4}$$

For $B \to \infty$, $\varepsilon_{33} \to 0$ and $t_{33} \approx \nu t_{11}$ so that (4) transforms to

$$t_{ij}(z;B\to\infty) = \begin{pmatrix} t_{11}(z;B\to\infty) & 0 & 0 \\ 0 & 0 & 0 \\ 0 & 0 & \nu\, t_{11}(z;B\to\infty) \end{pmatrix}. \tag{5}$$

Therefore, in the case $B \to \infty$, the tensor depends uniquely on t_{11}, and can be adequately considered as the reference parameter of constraint, as stated in the bi-parametric approaches. However, for a real B (notably for $B < B_{\min}$), the suitable expression for the t_{ij} tensor is (4). As a result, the t_{33} value is, in general, influenced by t_{11} and ε_{33} both depending on the specimen thickness B.

3. NUMERICAL CALCULATION OF THE COMPONENTS t_{11} AND t_{33} OF THE t_{ij} TENSOR

Different techniques can be applied for the calculation of the t_{ij} tensor components [5]. A direct derivation from the stress distribution, although feasible, is prone to inaccuracies in the extrapolation to the crack front. Instead, t_{11} can be determined using the interaction integral proposed by Nakamura-Parks [6]. Once t_{11} and ε_{33} are known, t_{33} can then readily be obtained from (3).

3.1 Model description

Cracked plates of different thickness B, crack depth ratios a/W and Poisson's ratios have been analysed using the FEM to check the validity of the theoretical derivations. The interest was focussed on the influence of the above parameters on the t_{11} and t_{33} components of the t_{ij} tensor. In this work, the analysis is restricted to plates with a straight crack front and mode-I loading. A linear elastic material with Young´s modulus $E = 207$ GPa and Poisson's ratio $\nu = 0.3$, unless otherwise stated, is considered for the numerical model as shown in Fig. 1. Fourteen different thicknesses $B = 0.1$, 0.2, 0.5, 1, 2, 5, 10, 20, 35, 50, 75, 100, 200, 400 mm and four different crack depth ratios $a/W =$ 0.1, 0.3, 0.5 and 0.7 were considered for the calculations aiming at studying the effect of thickness and crack length. A constant width $W = 50$ mm and height $H = W$ is assumed throughout the calculations and a uniform stress $\sigma = 1$ MPa is applied on the top side of the plate in all cases. 20-node isoparametric elements with 3x3x3 integration points are considered. The discretization in the transverse direction comprises 50 elements.

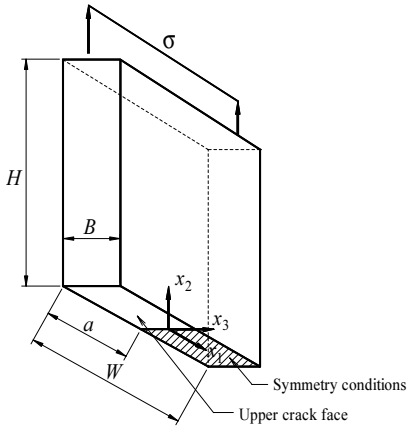

Figure 1. Geometric model of the cracked plates.

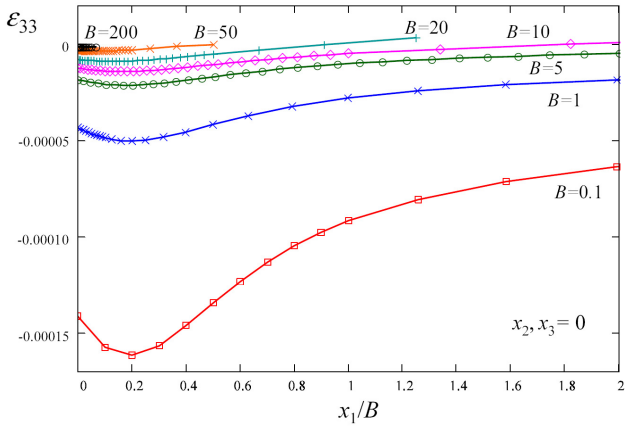

Figure 2. Normalized midplane variation of ε_{33} along the x_1-axis.

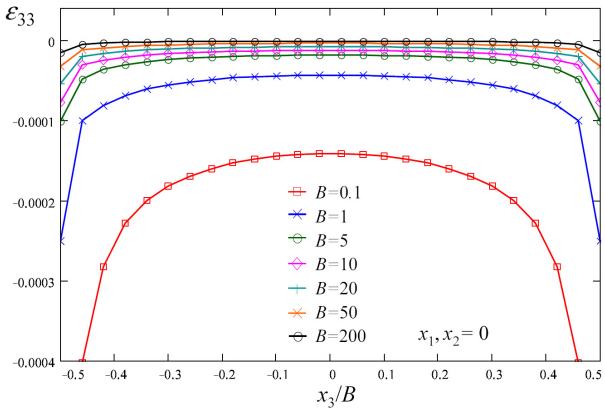

Figure 3. Normalized through-thickness variation of ε_{33} along the crack front.

3.2 Out-of-plane strain ε_{33}

Firstly, the out-of-plane strain ε_{33} for the different thicknesses was calculated at the midplane of the plate as a function of the normalized distance to the crack front in the x_1 direction (see Fig. 2). The same magnitude is depicted in Fig. 3 this time as a function of the normalized location x_3/B at the crack front. As shown, the results confirm the non-nullity of ε_{33} along the crack front in the case of plates of finite thickness. The greatest contraction is reached at a distance of about $x_1/B \approx 0.2$ ahead of the crack front.

3.3 Constraint functions

The constraint functions $\psi_{ij}(r;B)$ represent the stress intensity fields in the direction of the prospective crack propagation ($\theta = 0$ for mode-I):

$$\psi_{ij}(r;B) = \sqrt{2\pi r}\ \sigma_{ij}(r,\theta;B)\big|_{\theta=0} \qquad (6)$$

At the crack front, i.e. for $r \to 0$, the constraint functions ψ_{ij} converge to the respective stress intensity tensor components k_{ij}. This is shown in Fig. 4 with plots for ψ_{11} and ψ_{22} normalized by $k_{11} = k_{22} = K_I$ at the mid-plane $x_3 = 0$ for the plate $B = 1$ mm. As expected, the constraint functions converge to 1 when $r \to 0$. For the out-of-plane constraint function ψ_{33} it is verified that converges to $k_{33} = 2\nu K_I$ when $r \to 0$. Thus, the constraint functions supply relevant information on the three-dimensional near stress field distribution.

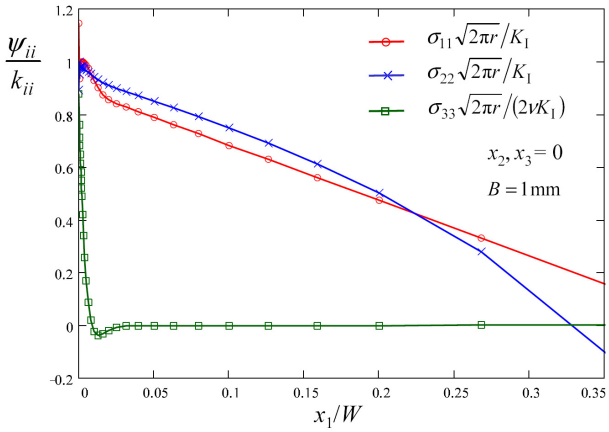

Figure 4. Mid-plane variation of ψ_{ii} (normalized by k_{ii}) along the x_1 axis.

For increasing r, the constraint function ψ_{33} shows a particularly noticeable decay rate, pointing out its close connection with the loss of constraint. This decay rate is strongly dependent on the specimen thickness. The constraint function ψ_{33} gets normalized with respect to B, when a dimensionless distance x_1/B to the crack front is used as abscissa (see Fig. 5), showing the same behaviour of the decay regardless the specimen thickness. A characterization of the loss of constraint is thus possible through the simultaneous consideration of the higher tensor terms of the Williams expansion as a whole, i.e. not only through the sole consideration of the T-stress as suggested by current approaches but also considering the out-of-plane component t_{33}.

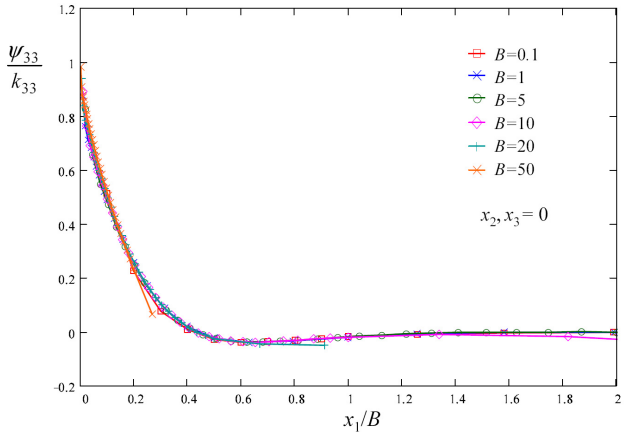

Figure 5. Constraint curves ψ_{33} (normalized by k_{33}) for different B vs. the dimensionless distance x_1/B.

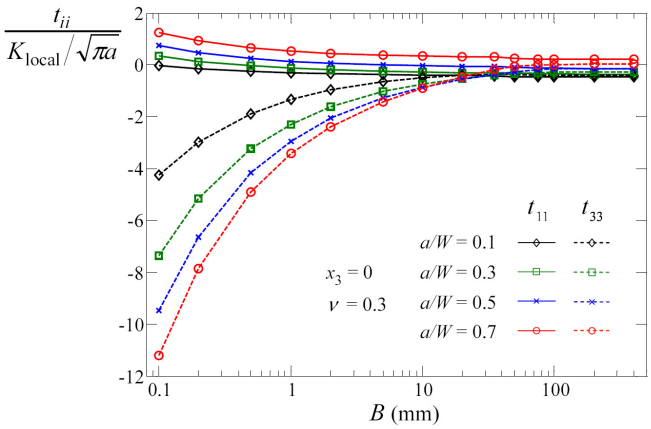

Figure 6. Variation of t_{11} and t_{33} with B and a/W at the mid-plane $x_3 = 0$.

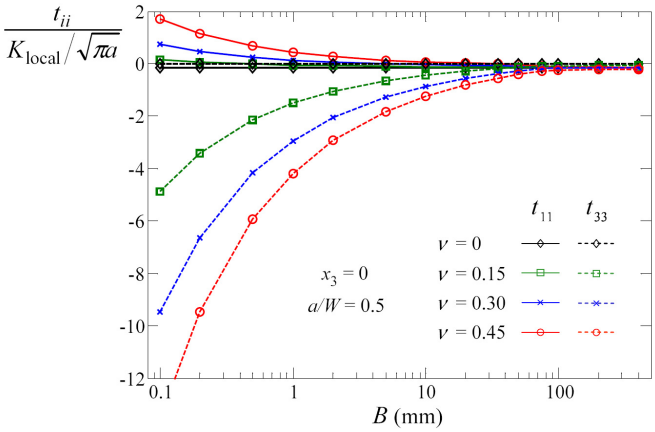

Figure 7. Variation of t_{11} and t_{33} with B and the Poisson's coefficient ν at the mid-plane $x_3 = 0$.

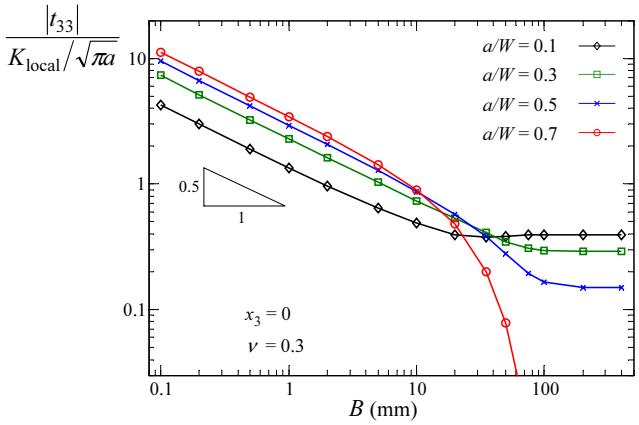

Figure 8. Log-log plot of normalized $|t_{33}|$ vs. B.

3.4 Calculation of t_{11} and t_{33}

Fig. 6 and 7 show the results of t_{11} and t_{33} calculated at the mid-plane $x_3 = 0$ for the fourteen thicknesses B, four a/W ratios and four Poisson's coefficients. The results are normalized by an equivalent stress calculated from $K_{\text{local}}/(\pi a)^{0.5}$, where K_{local} is the mode-I SIF evaluated at that particular location of the crack front ($x_3 = 0$) using an equivalent domain integral for J. According to [4], a unique constant relationship between J and K_{local} exists, i.e. $K_{\text{local}} = (J_{\text{local}}\, E/(1-\nu^2))^{0.5}$, which is independent of the specimen thickness. Two features merit comment: Firstly, t_{33} is always negative (it is a compressive stress) whereas t_{11} can change its sign for small values of a/W (t_{11} tends to be negative for small a/W ratios and large B). This means that the t_{11} and t_{33} values run in opposite trend for decreasing specimen thicknesses. Secondly, the absolute magnitude of t_{33} tends to be approximately one order of magnitude greater than the magnitude of t_{11} pointing out that, in general, the effect of t_{33} cannot be neglected. Moreover, the magnitudes of t_{11} and t_{33} increase for small B, for large a/W and for large ν. As expected, the sensitivity of t_{11} to the ratio a/W is greater than to the thickness B, since t_{11} is an in-plane stress. Note that, in general, t_{11} changes with B (contrary to what it is often stated in the literature) although this dependency is small for the case $a/W = 0.1$. The magnitude of t_{33} is much more sensitive to both B and a/W. Only for very large thicknesses we can observe that t_{33} is small and almost independent of a/W.

Since all the constraint effects present in 3D crack problems are ultimately due to existence of Poisson's ratio effects, its influence is very significative [6], see Fig. 7. Of course, for the case $\nu = 0$, there is no thickness effect and the plate behaves self-similarly throughout the thickness. Note that $t_{33} = 0$ because there is no Poisson contraction in the thickness direction. In this case, t_{11} is not zero and coincides with the value calculated for a 2D plate (the T-stress, like the SIF, is independent of ν and of the limiting 2-D case, plane stress or plane strain, assumed).

Fig. 8 shows a log-log plot of the absolute value of t_{33} (normalized by $K_{\text{local}}/(\pi a)^{0.5}$) versus thickness B. It can be observed that the values fit very well to a straight line of slope −0.5 for small thicknesses (up to approximately $B = 5$ mm). Therefore, a normalization of t_{33} at the mid-plane for small thicknesses and a given a/W ratio, can be achieved using:

$$\frac{t_{33}}{K_{\text{local}}/\sqrt{\pi\, a}}\sqrt{B} = \text{constant} \qquad (7)$$

This relationship enables the approximate calculation of t_{33} for other B provided a computation for a certain B is known and the thicknesses are small. For thicknesses larger than $B = 5$ mm, the effect of the boundaries at $x_1 = \pm W/2$ increases due to the greater relative proximity of these borders and the agreement with a straight line is lost.

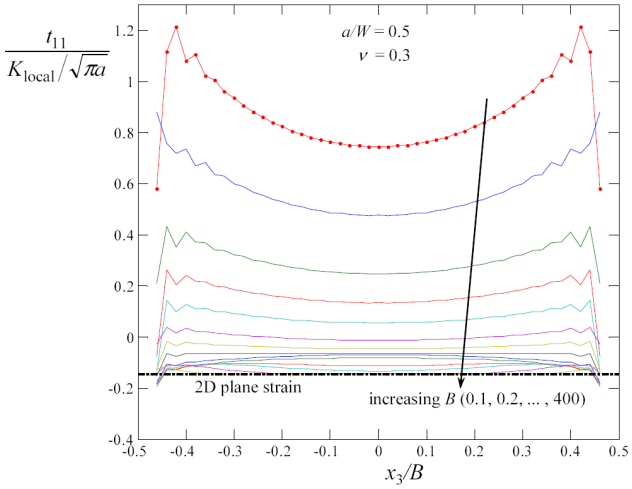

Figure 9. Through-thickness variation of t_{11} along the crack front for different thicknesses B.

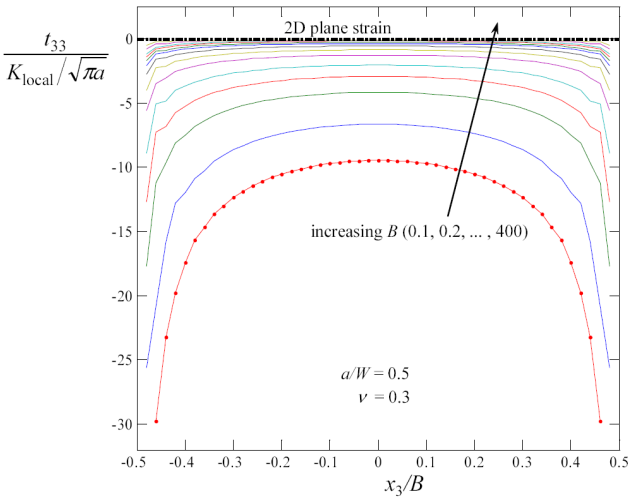

Figure 10. Through-thickness variation of t_{33} along the crack front for different thicknesses B.

In Figs. 9 and 10, the through-thickness variation of t_{11} and t_{33} for the set of fourteen thicknesses is plotted versus the normalized location x_3/B along the crack front. As for the mid-plane location analyzed in previous sections, we can observe that t_{11} and t_{33} clearly increase as $B \to 0$ for all points on the crack front. In general, the magnitude at the rest of the crack front is even greater than at mid-plane. As expected t_{11} and t_{33} converge to the 2D plane strain values as $B \to \infty$. This implies a flattening of the curves, decreasing the range of influence of the corner singularities at $x_3/B = \pm 0.5$ for large B.

Note that the value of t_{33} in the 2D plane strain problem, although small, is not zero but $t_{33} = \nu t_{11}$ as commented in Section 2. The computations of t_{11} and t_{33} in the vicinity of the free surfaces must be interpreted with caution, since ε_{33} is singular at the corner intersections and is not well calculated using finite elements. The singular behaviour of ε_{33} in these zones affects in several ways: first, the computation of the interaction integral used to compute t_{11} tends to diverge [6]; second, the calculations of t_{11} and t_{33} through the interaction integral and Eq. (3), respectively, involve an explicit summation of ε_{33} which tends to be singular. Moreover, the validity of the extraction field used in the interaction integral (see [6]) is questioned, as the auxiliary fields corresponding to a line-load of unit magnitude assume a plane strain behaviour. In our opinion, the computation of t_{11} and t_{33} near the free surfaces still requires further research.

5. TRIAXIALITY AND CONSTRAINT

Due to the lack of a satisfactory model to analyse the constraint problem in its whole complexity, some confusion has been observed in the literature referring to triaxiality and constraint. According to the analysis performed in this work, we can state that although having some similitude both definitions represents different concepts. The consideration of the constraint curves helps to understand this question. The study of the influence of the specimen thickness proves that triaxiality is ubiquitous: it is always present in any crack stress distribution irrespective of the specimen thickness B, both in thick specimens (when $B >> B_{min}$) as well as in thin specimens (when $B << B_{min}$) when analyzed sufficiently close to the crack front. Nevertheless, these dissimilar situations clearly represent two opposite constraint states, as shown by the distinct values of the apparent fracture toughness experimentally obtained in both cases. Loss of constraint means limited triaxiality extension but by no means an “absence of triaxiality”.

Applying the constraint function concept to the analysis of the phenomenon allows us to give an adequate interpretation of the constraint role and to understand the differences and affinities of the two limiting cases $B \to 0$ (not to be mistaken for plane stress) and $B \to \infty$. Outside from the out-of-constraint zone we can properly speak of 2-D conditions. Though the corresponding constraint curves are qualitatively similar (or even identical after being normalized) their quantitative differences are important depending on the geometric relations. The constraint curves define the extension of the constraint zone.

Since the structure of the k_{ij} has been demonstrated to be independent of the specimen thickness, an explanation of the differences arising in the apparent fracture toughness for specimens showing different thicknesses must be found in the local fracture criterion, based on a stress fracture criterion at a certain distance

of the crack front rather than in a stress intensity factor criterion, the former being influenced by the existing constraint, i.e. the t_{ij} tensor and the extension of the plastic zone.

6. CONCLUSIONS

The main conclusions arising from this work are the following:

- Current biparametric approaches ignore the tridimensional nature of the constant term in Williams expansion so that they cannot describe the influence of the different triaxiality degrees that exist in real specimens of finite thickness. The T-stress alone, i.e. t_{11}, does not give information about the loss of constraint as a whole comprising both in- and out-of-plane effects.

- The present approach proposes the use of the tensor t_{ij} with components t_{11} and t_{33}, and enables the proper definition of complex constraint states arising in real specimens. With this proposal, the effects of both crack length and specimen thickness on the apparent fracture toughness can be addressed.

- The validity of the biparametric approach for specimen thicknesses greater than $B_{\min}$ can be explained as an special case in which t_{33} becomes νt_{11} due to the condition $\varepsilon_{33} \approx 0$, so that t_{ij} can be expressed solely in terms of t_{11}. On the contrary, t_{ij} depends on both t_{11} and t_{33} for thinner specimens.

- It is also shown that t_{11} depends on other factors, such as the specimen thickness B.

- The interdependence among t_{11}, t_{33} and ε_{33} has been analytically derived.

- The constraint curves ψ_{ij} facilitate the conceptual comprehension of the loss of constraint and can be used for a quantitative assessment.

- The numerical calculations prove that specimen thickness B and crack depth ratio a/W exert an influence on the results of both components of the t_{ij} tensor, i.e. on t_{11} and t_{33}, the latter being more sensitive to those factors. As a result, the influence on the apparent fracture toughness cannot be merely attributed to the in-plane component.

- It is possible to normalize t_{33} for small specimen thicknesses, enabling an easy evaluation of the thickness influence on the t_{33} stress.

ACKNOWLEDGEMENTS

The authors gratefully acknowledge the financial support given by the DGICYT of the Spanish Ministry of Science and Innovation (Projects DPI2007-66995-C03-02 and DPI2007-66903-C02-01) and by FICYT (Project IB08-171).

REFERENCES

[1] Seitl S., Knésl Z., *Two parameter fracture mechanics: fatigue crack behaviour under mixed mode conditions*, Eng. Fracture Mech. 72, 857-865, 2008.

[2] Betegón C., Hancock J., *Two- parameter characterization of elastic-plastic crack-tip fields.* J. Appl. Mech. Transactions of the ASME, 113, 104-110, 1991.

[3] Fernández Canteli A., Castillo E., Fernández Zúñiga D., *Linear-elastic fracture mechanics based criteria for fracture including out-of-plane constraint effect*, Submitted to Theoretical and Applied Fracture Mechanics, 2009.

[4] Giner E., Fernández Zúñiga D., J. Fernández Sáez, Fernández Canteli A., *On the J_{x1}-integral and the out-of-plane constraint in a 3D elastic cracked plate loaded in tension,* Submitted to Int. J. Solids Structures, 2009.

[5] Fernández Zúñiga D., Kalthoff J.F., Fernández Canteli A., Grasa J., Doblaré M., *Three-dimensional finite element calculations of crack tip plastic zones and K_{Ic} specimen size requirements*, ECF 15, Stockholm, 11-13 August 2004

[6] Nakamura T., Parks D.M., *Determination of elastic T-stress along three-dimensional crack fronts using an interaction integral*, Int. J. Solids Structures, 29, 1597-1611, 1992.

[7] Kwon S., Sun C., *Characteristics of three-dimensional stress fields in plates with a through-the-thickness crack*, Int. J. Fracture, 104, 291-315, 2000.

[8] Williams M.L., *On the stress distribution at the base of a stationary crack*. J. Appl. Mech., 24, 109-114, 1957.